Supporting information: Sulfidation kinetics of copper oxide nanoparticles

Alexander Gogos[a], Basilius Thalmann[a], Andreas Voegelin[a] and Ralf Kaegi[a],*

[a] Eawag, Swiss Federal Institute of Aquatic Science and Technology,

Überlandstrasse 133, CH-8600 Dübendorf

* Corresponding author. Tel.: +41 (0)58 765 52 73; e-mail: ralf.kaegi@eawag.ch.

3

Tables

Table S1: Summary of experimental conditions including fitted pseudo first-order reaction rate constants k' and calculated half-life times $t_{1/2}$.

CuO [μM]	HS⁻ [μM]	HS⁻:Cu	k' [min⁻¹]	$t_{1/2}$ [min]
7.7	26.4	3.4	0.127	5.83
7.7	42.2	5.4	0.225	3.08
7.7	52.8	6.8	0.281	2.46
7.7	63.4	8.2	0.407	1.70
7.7	79.2	10.2	0.620	1.12
7.7	105.6	13.6	0.636	1.09

Table S2: Hydrodynamic size and ζ-potential at different concentrations of the CuO NP in the Tris-buffered medium at pH 8.

Concentration CuO NP	Concentration Tris-buffer	Hydrodynamic diameter [nm]	Standard deviation	RSD %	ζ-potential [mV]	Standard deviation	RSD %	PDI	Standard deviation	RSD %
1 mM	50 mM	302.7	11.3	3.7	-40.2	2.2	5.5	0.36	0.03	7.5
0.1 mM	5 mM	233	4.9	2.1	-46.8	0.9	1.9	0.38	0.1	26.3
0.01 mM	0.5 mM	430	18	4.2	-46.9	2.3	4.9	0.48	0.1	20.8

Table S3: Cu and HS⁻ concentrations in waste water (WW) from selected references.

Reference	µM Cu in WW	Reference	µM HS⁻ in WW	Resulting HS⁻:Cu range
Böhm 2001 [1]	0.79 - 5.5	Liu 2011 [2]	300	3.3 – 700
Karvelas 2003 [3]	0.69 - 1.8	Sharma 2014 [4]	30 - 480	
Wang 2014 [5]	1.2 - 9.1			

Table S4: LCF results for different time points of the reaction of CuO NP and HS⁻ (1.3 mM CuO, HS⁻:Cu 4.14), obtained from XANES spectra between 8964 and 9064 eV.

Time [min]	rfactor	CuS primitive Pattrick et al. weight (error)	CuO NP weight (error)	CuS (covellite) weight (error)	Cu^{2+}(aq) weight (error)	Total
0	0.0E+00	0.00 (0.00)	1.00 (0.00)	0.00 (0.00)	0.00 (0.00)	1.00
0.25	2.2E-04	0.43 (0.02)	0.38 (0.01)	0.18 (0.02)	0.03 (0.01)	1.02
5	1.3E-04	0.46 (0.02)	0.22 (0.01)	0.30 (0.02)	0.03 (0.01)	1.01
15	1.7E-04	0.46 (0.02)	0.14 (0.01)	0.39 (0.02)	0.02 (0.01)	1.01
60	2.7E-04	0.25 (0.02)	0.09 (0.01)	0.67 (0.02)	0.00 (0.01)	1.01
180	6.5E-04	0.00 (0.03)	0.09 (0.02)	0.93 (0.04)	0.00 (0.01)	1.02
4320	3.5E-04	0.00 (0.02)	0.09 (0.01)	0.93 (0.03)	0.00 (0.01)	1.02

Table S5: LCF results for different time points of the reaction of CuO NP and HS$^-$ (1.3 mM CuO, HS$^-$:Cu 4.14), obtained from EXAFS spectra between 3 and 6 Å^{-1}.

Time [min]	rfactor	CuS primitive Pattrick et al. weight (error)	CuO NP weight (error)	CuS (covellite) weight (error)	Cu^{2+}(aq) weight (error)	Total
0	0.0E+00	0.00 (0.00)	1.00 (0.00)	0.00 (0.00)	0.00 (0.00)	1.00
0.25	1.6E-02	0.69 (0.00)	0.31(0.00)	0.00 (0.00)	0.00 (0.00)	1.00
5	9.3E-03	0.73 (0.05)	0.25 (0.02)	0.12 (0.06)	0.05 (0.04)	1.15
15	6.7E-03	0.68 (0.05)	0.14 (0.02)	0.27 (0.05)	0.07 (0.03)	1.16
60	2.2E-02	0.56 (0.00)	0.00 (0.00)	0.69 (0.00)	0.05 (0.00)	1.32
180	6.3E-03	0.30 (0.00)	0.00 (0.00)	1.00 (0.00)	0.03 (0.00)	1.33
4320	2.6E-02	0.00 (0.00)	0.00 (0.00)	1.00 (0.00)	0.19 (0.00)	1.19

Figures
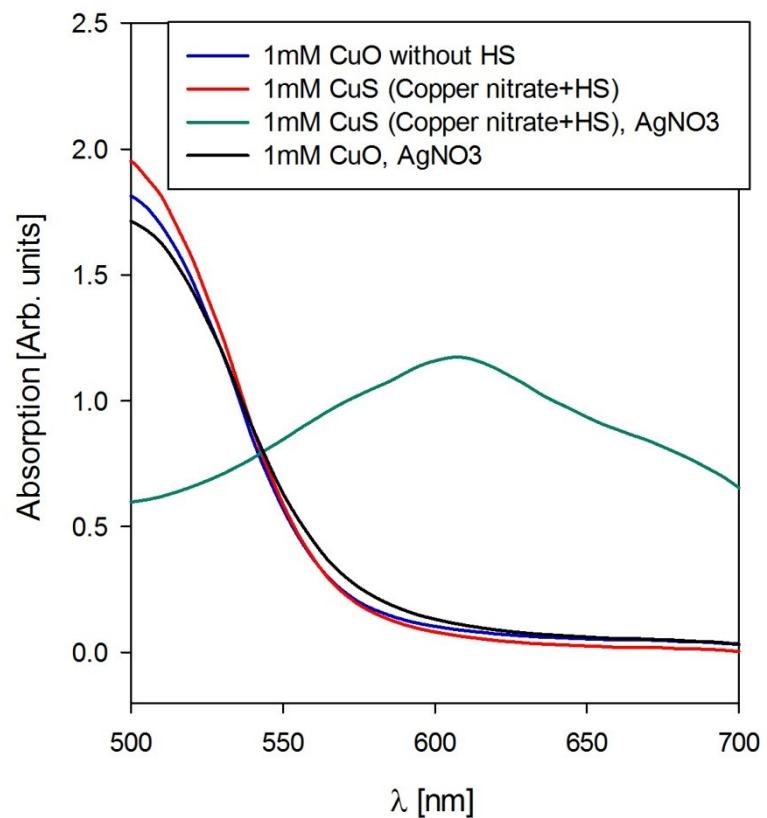
Fig. S1: UV-Vis spectra after Zincon addition showing (i) CuO without HS⁻ and AgNO$_3$ addition (blue line), (ii) Synthetic CuS (copper nitrate + HS⁻) without AgNO$_3$ addition (red line), (iii) Synthetic CuS (copper nitrate + HS⁻) with AgNO$_3$ addition (green line) and (iv) CuO without HS⁻ and additional AgNO$_3$ (black line). Experiments were conducted at 1mM CuO/CuS and at a molar Ag : Cu ratio of 10. 94% of the added 1mM Cu were recovered after AgNO$_3$ addition to 1mM CuS (green line, determined using the peak absorption at 600 nm (1.15) and external calibration).
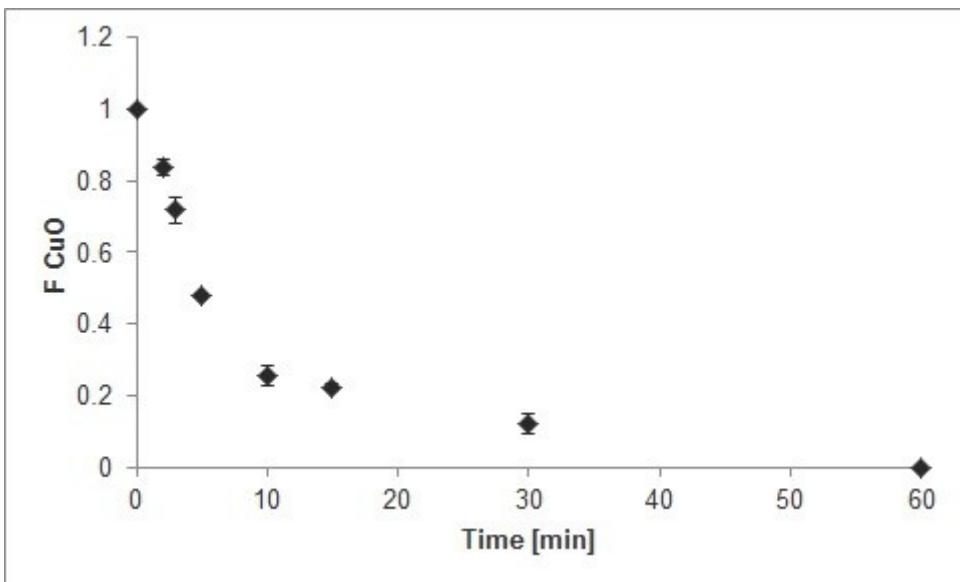
Fig. S2: Decrease of the CuO fraction determined using the colorimetric method (CuO 7.7 µM, HS$^-$:Cu 3.4). Standard deviations of three replicate measurements are indicated by the error bars.
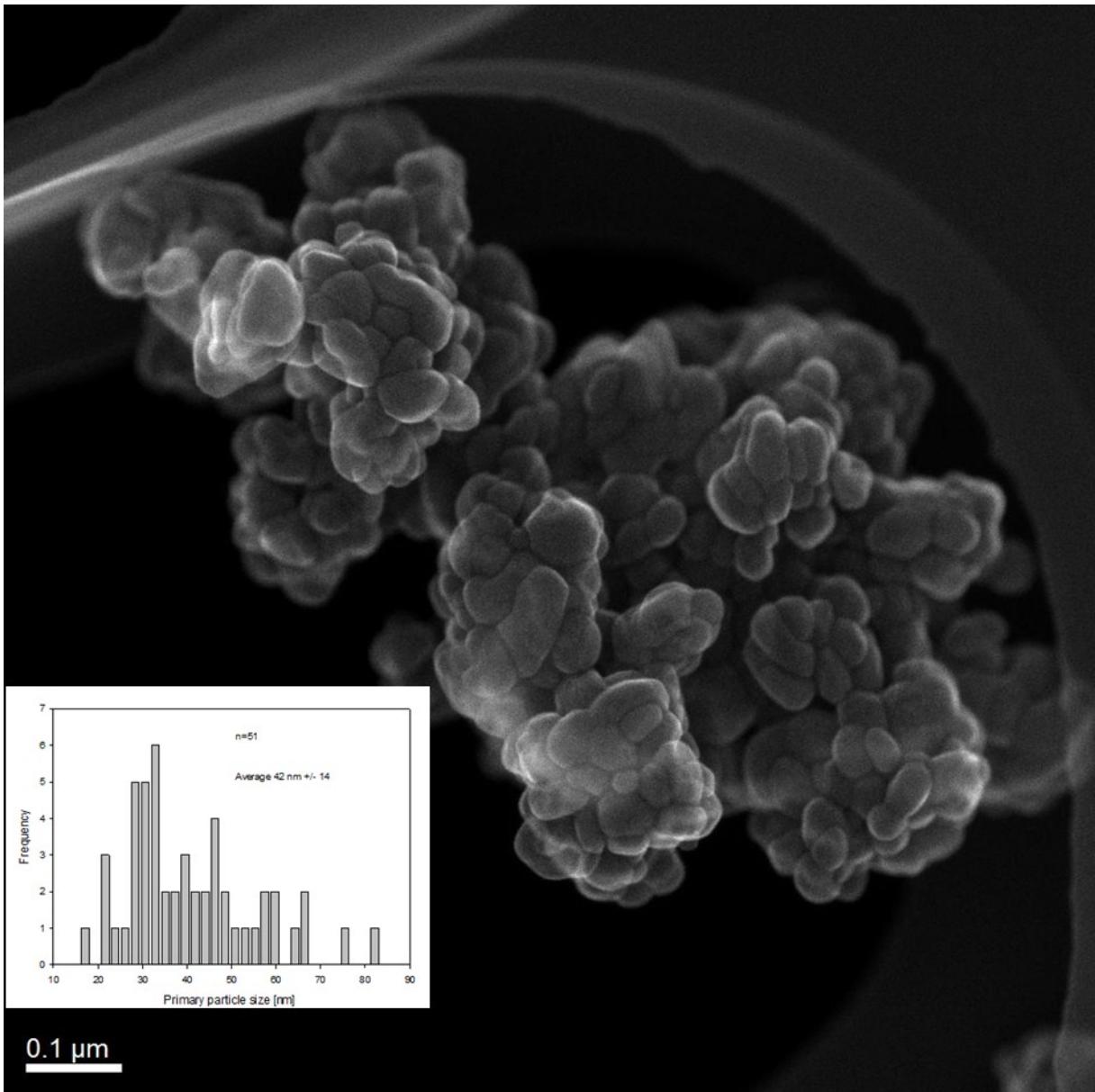
Figure S3: STEM-SE image of the CuO NPs together with the size distribution calculated from 51 individual NPs.
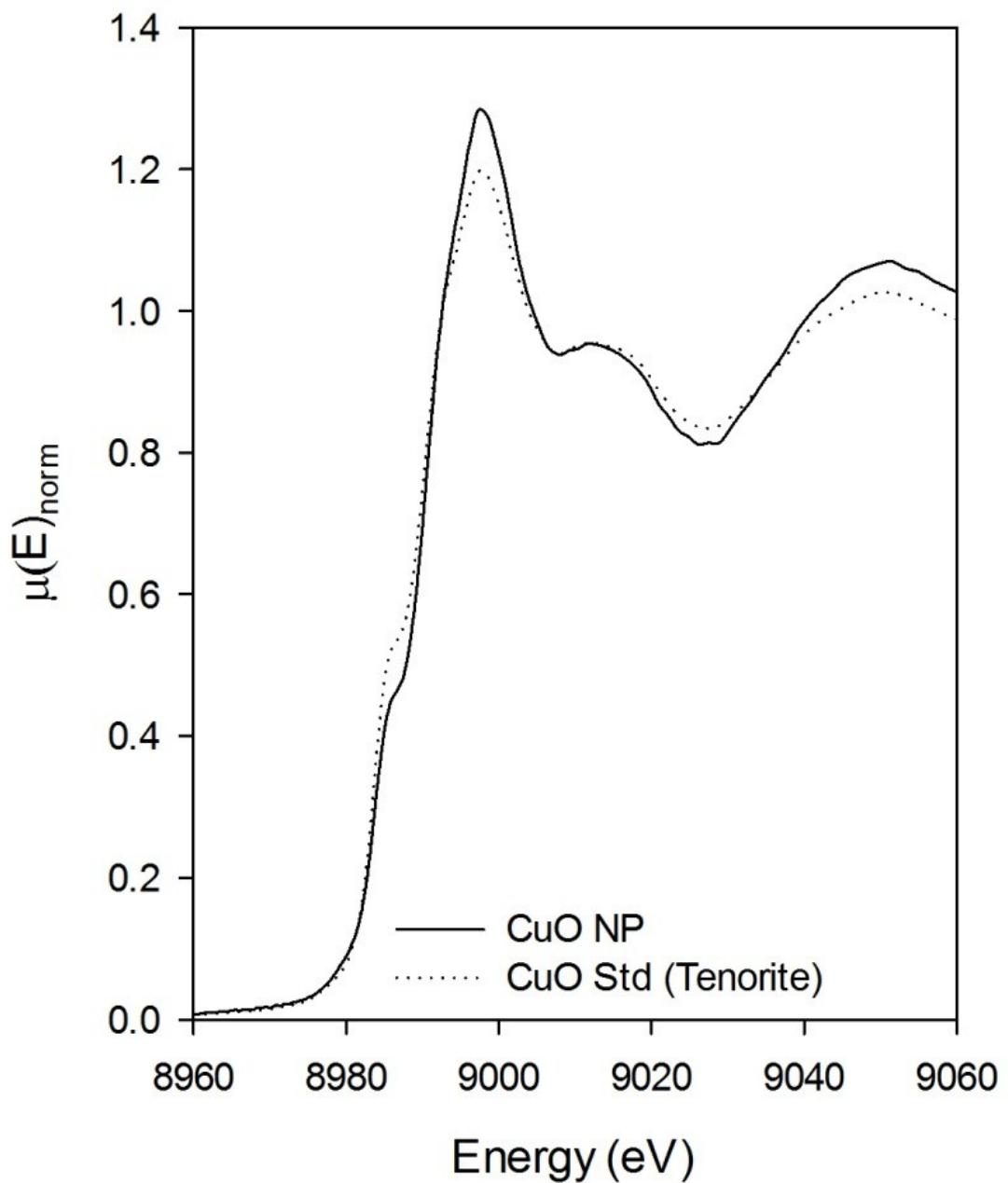
Figure S4: Normalized XANES spectra of CuO NP (solid line) and CuO tenorite (dotted line).
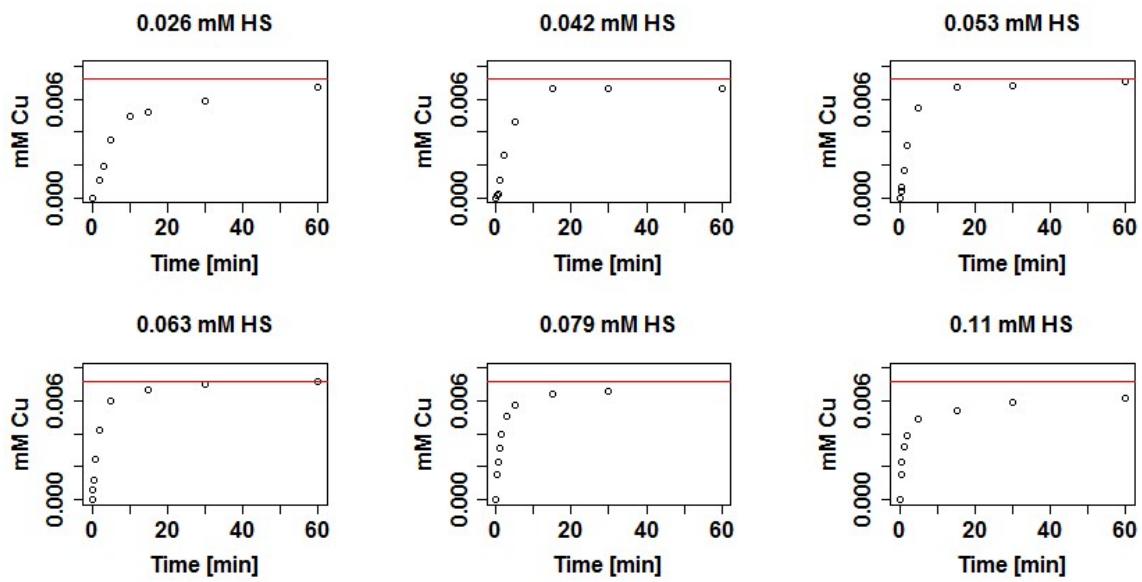
Fig. S5: Increase of Cu^{2+} determined using the colorimetric method at initial CuO of 7.7 µM (solid red line) and different HS^- concentrations (indicated above each graph) over time.
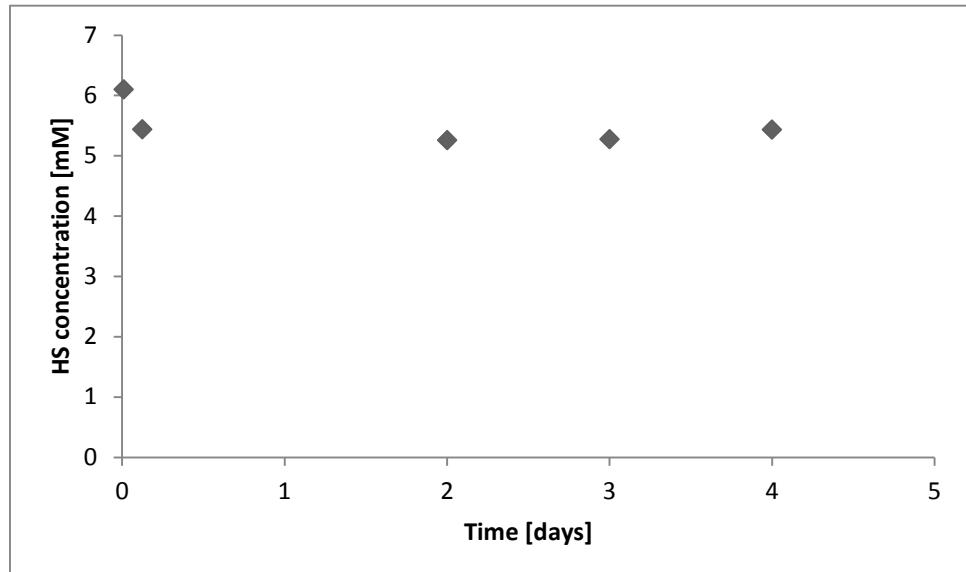

Figure S6: HS^- concentrations in the Tris-buffered reaction medium (pH 8.0) over time, determined using the iodometric method in absence of CuO NPs.

1.3mM CuO, 4.14xHS, pH8
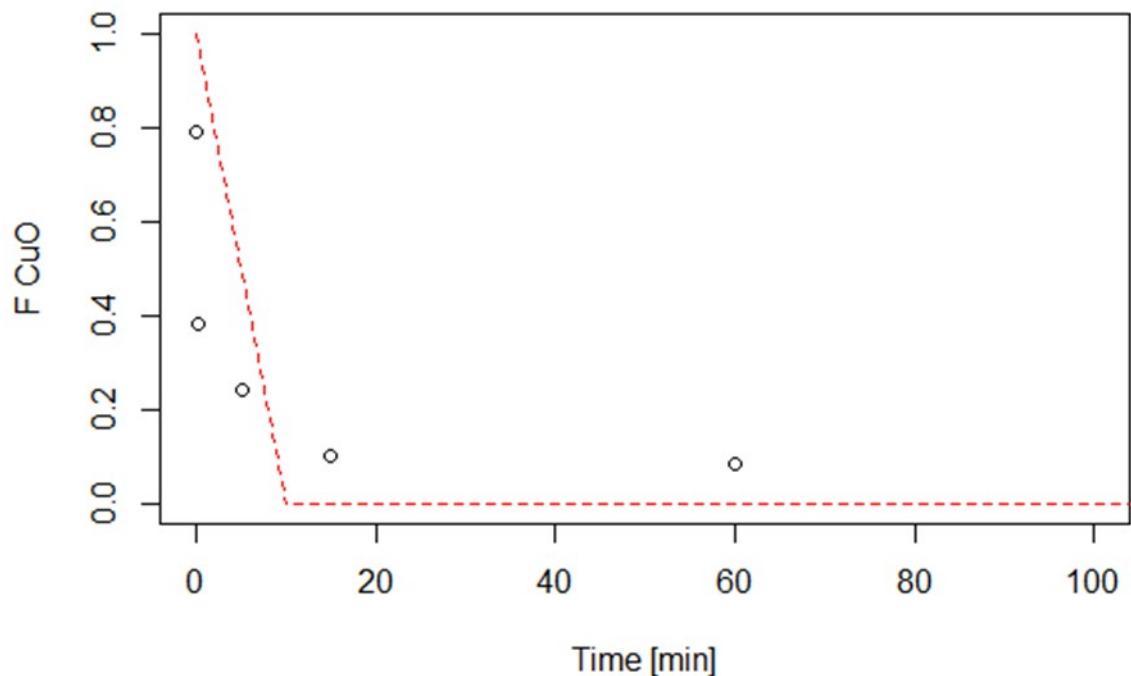
Fig. S7: Fraction of CuO determined at increasing reaction time using LCF analysis of XANES spectra. The dashed red line represents the pseudo first-order model fit derived from non-linear regressions of the experimental data. The reaction rate k' determined from this fit was 3.8 min^{-1}.
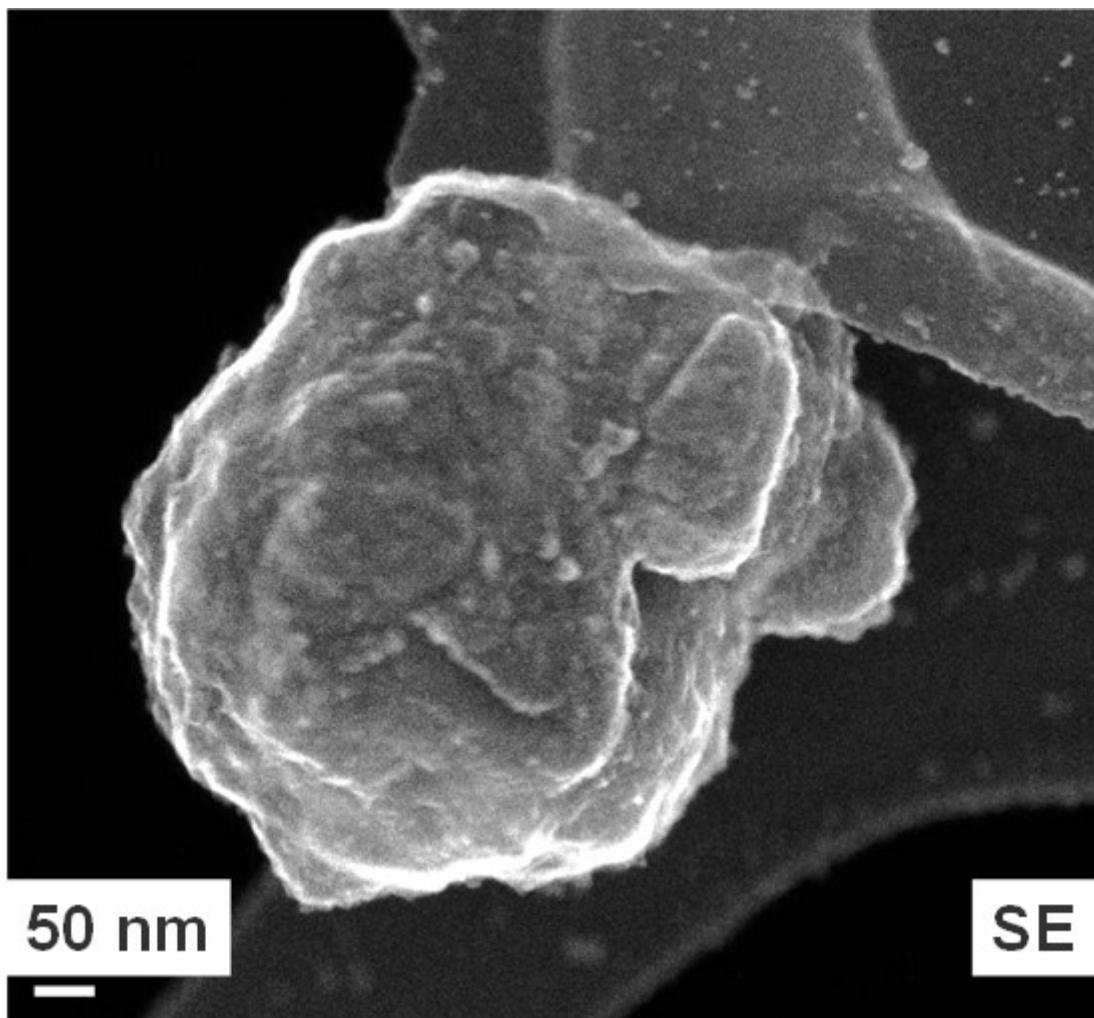
Fig. S8: STEM-SE image showing particles after 5 min reaction time (1.3 mM CuO, HS⁻:Cu 4.14). Small particles (< 15nm) are attached to the transformed CuO NP.
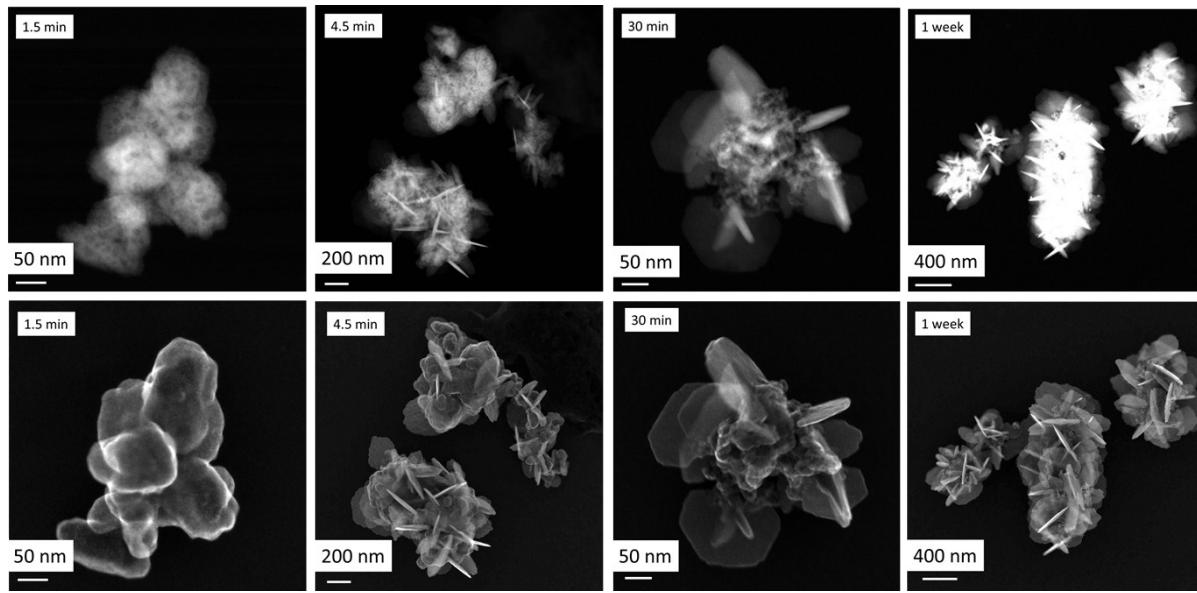
Figure S9: STEM – HAADF (upper panel) and corresponding SE (lower panel) images showing agglomerated particles at increasing reaction times (7.7 µM CuO, HS⁻:Cu 3.4).

References

1. E. Böhm, T. Millenbrand, F. Marscheider-Weidemann, C. Schemp, S. Fuchs and U. Scherer, *Bilanzierung des Eintrags prioritärer Schwermetalle in Gewässer*, Umweltbundesamt (Federal office for the environment), Germany, 2001.
2. J. Liu, K. G. Pennell and R. H. Hurt, *Environ. Sci. Technol.*, 2011, **45**, 7345-7353.
3. M. Karvelas, A. Katsoyiannis and C. Samara, *Chemosphere*, 2003, **53**, 1201-1210.
4. K. Sharma, N. Derlon, S. Hu and Z. Yuan, *water research*, 2014, **49**, 175-185.
5. H. Wang and Z. J. Ren, *Water Research*, 2014, **66**, 219-232.